

Distributed AC Optimal Power Flow: A Scalable Solution for Large-Scale Problems

Xinliang Dai, Yuning Jiang*, Yi Guo, Colin N. Jones, Moritz Diehl, Veit Hagenmeyer

Abstract—This paper introduces a novel distributed optimization framework for large-scale AC Optimal Power Flow (OPF) problems, offering both theoretical convergence guarantees and rapid convergence in practice. By integrating smoothing techniques and the Schur complement, the proposed approach addresses the scalability challenges and reduces communication overhead in distributed AC OPF. Additionally, optimal network decomposition enables efficient parallel processing under the single program multiple data (SPMD) paradigm. Extensive simulations on large-scale benchmarks across various operating scenarios indicate that the proposed framework is 2 to 5 times faster than the state-of-the-art centralized solver IPOPT on modest hardware. This paves the way for more scalable and efficient distributed optimization in future power system applications.

Index Terms—Distributed optimization, optimal power flow, large-scale problems.

I. INTRODUCTION

The AC optimal power flow (OPF) problem is one of the most practically important optimization problems in electric power systems engineering [1]. It is generally NP-hard, even for radial power grids [2], [3]. Traditionally, this problem is solved by using centralized approaches, primarily for long-term scheduling and planning purposes [1]. However, the ongoing energy transition presents new challenges for these centralized paradigms. The increasing integration of distributed energy resources (DERs) introduces rapid fluctuations in energy supply and demand, complicating the management of transmission and distribution systems and requiring enhanced coordination among system operators [4]. Additionally, as more controllable devices are installed in power systems, centralizing all data not only raises significant privacy concerns but also places greater demands on communication infrastructure [5].

In response to these challenges, distributed optimization offers an efficient alternative for coordinating geographically dispersed systems, allowing independent operation and effective collaboration through limited information sharing. Potential advantages of distributed optimization algorithms in power systems include [4]–[6]:

- **Scalability:** Distributed algorithms decompose large, complex problems into smaller subproblems. This enables fast computations and makes the approach scalable.

- **Privacy and Sovereignty Preservation:** With distributed optimization, data privacy is better preserved because detailed information, such as grid configurations or customer usage behaviors: does not need to be shared. Each entity can maintain the confidentiality of its own data, which is crucial in collaborations where different entities own and operate separate parts of the system.
- **Robustness:** Distributed approaches enhance system reliability and resiliency by mitigating the risk of single-point cyber failures that centralized systems are prone to.
- **Adaptability:** These algorithms adapt more quickly to network topology and infrastructure changes without requiring a complete system overview. This enables flexible reconfiguration of the system when new components are added, or existing ones are modified.

Comprehensive surveys on distributed optimization can be found in [5]–[8].

TABLE I: Distributed problem formulation of AC optimal power flow

Type	Network	Topology	Model	Problem Type
I	Partitioned	Generic	BIM	Nonconvex
II	Merged	Generic	BIM	Nonconvex
III	Merged	Stellate	BIM	Nonconvex
IV	Merged	Stellate	Hybrid	Partially Convexified
V	Merged	Stellate	BFM	Convexified

TABLE II: Distributed optimization for solving large-scale AC OPF

Ref.	Type	Algorithm	Global/Local Convergence	N^{bus}	Execution	Speed	Accuracy
[9], [10]	IV	DCC	Local	10^3	Sequential	+++	+++
[11]–[13]	V	ADMM	-	10^3	Sequential	+	+
[14]	III	Distr. IPM	Local	10^7	Parallel	+++	+++
[15]	II	Distr. IPM	Local	10^2	Sequential	+++	+++
[16]	II	ALADIN	Global	10^3	Sequential	+++	+++
[17]	I	ADMM	-	10^2	Sequential	+	+
[18]	I	ADMM	-	10^3	Sequential	+	+
[19]	I	ADMM	-	10^4	Sequential	+	+
[20], [21]	I	ADMM	Global	10^4	Parallel	+	+
[22], [23]	I	ALADIN	Global	10^2	Sequential	+++	+++
[24]	I	ALADIN	Global	10^1	Sequential	+++	+++
[25]	I	ALADIN	Global	10^2	Distributed	++	+++

To tackle the nonconvex AC OPF problems in a distributed fashion, existing approaches often exploit specific network structures. For instance, some studies [11]–[13] restricted to fully radial networks (Type V), which enables convex relaxations based on the branch flow model (BFM). Other studies focus on specific integrated transmission-distribution (ITD) systems, where multiple distribution networks are connected to a single transmission network in a star-like pattern (Types III and IV in Table I). These approaches use master-worker-splitting [26], where each worker solves a decoupled subprob-

*corresponding: yuning.jiang@ieee.org

XD and VH are with the Institute for Automation and Applied Informatics, the Karlsruhe Institute of Technology.

YJ and CJ are with Automatic Control Laboratory, EPFL.

YG is with Urban Energy Systems Laboratory, Swiss Federal Laboratory for Materials Science and Technology.

MD is with the Department of Microsystems Engineering (IMTEK) and Department of Mathematics, University of Freiburg

lem with fixed boundary variables, and the master system updates these variables iteratively based on local solutions. Notably, the master problem need not be convex, enabling meshed subnetwork to be modeled using the bus injection model (BIM) [9], [10]. Recent work [14] (Types III) removes the convexity requirement for worker subproblems entirely. Instead, scalability is enhanced via an interior point method that smooths feasible regions and implicit sensitivities within worker systems. However, these approaches rely on one central master problem, and their performance often depends on the master system's convergence properties. Although some studies have extended these techniques to more complex topologies (Type II) [15], [16], the testing is usually limited to standard IEEE cases with limited connecting lines, leaving the impact of coupling density and their applicability to real-world systems unknown.

Instead of merging, we partition the overall network into multiple subgrids in the present paper, creating more complex and realistic coupling structures (Type I in Table I). These approaches reformulate the overall problems in standard distributed forms and use generic distributed optimization algorithms to solve them. Such methods can be easily extended to integrated transmission-distribution (ITD) systems, distribution systems, and other optimization and control problems in power systems. Among these, the Alternating Direction Method of Multipliers (ADMM) has gained significant attention. Early work by [17], [27] proposed regional decomposition but was limited to test cases up to one hundred buses. To improve scalability, [28] suggested partitioning grids based on power flow derivatives, making their approach feasible for larger problems in [18]. Further scalability improvements were achieved by [19] that introduced an acceleration scheme which enabled ADMM to solve the case13659 in MATPOWER [29]. Recent studies [20], [21] have bridged the theoretical gap by utilizing a two-level framework with global convergence guarantees for AC OPF, capable of solving the case30000 from the PGLib-OPF benchmark [30]. However, as a first-order optimization algorithm, the primary drawback of ADMM-type algorithms for nonconvex problems is the requirement for hundreds to thousands of iterations to achieve modest accuracy. Even if the accuracy is sufficient in practice, the intensive communication needed among distributed agents to solve one instance of the optimization problem requires an expensive communication infrastructure with high bandwidth and low delays.

To accelerate convergence, the Augmented Lagrangian-based Alternating Direction Inexact Newton method (ALADIN), first proposed in [31] for generic nonconvex distributed optimization problems, combines ideas from ADMM and sequential quadratic programming (SQP). This approach provides global convergence guarantees and achieves a locally quadratic convergence rate when the Hessian is properly selected. ALADIN was first applied to AC OPF problems in [22], [23], requiring only 26 iterations to reach around 10^{-5} accuracy for case300. As a generic nonlinear solver with convergence guarantees, the algorithm was first employed in a geographically distributed computing environment in [25]. This study highlights significant synchronization delays caused

by delivering the full KKT matrix information via network storage systems. In [24], further efforts were made to the reduction of communication effort by condensing derivatives using null space and Schur complement methods, but scalability remains limited. Although ALADIN has demonstrated good scalability in the absence of inequality constraints [4], [31], [32], its scalability is challenged due to its use of the active-set method, leading to combinatorial challenges [33, Ch. 15.2], as further noted in [16], [34].

Despite the theoretical advantages, critical issues of distributed optimization remain before its true value can be fully realized. This paper investigates generic distributed optimization for real-world, large-scale nonconvex problems, aiming to address these challenges as identified by [5]:

- **Convergence Speed:** Algorithms must be fast enough to handle rapid changes in grid conditions, but many current methods require thousands of iterations for acceptable accuracy, indicating the need for improved convergence rates.
- **Convergence Guarantees:** There is a need for theoretical frameworks that ensure convergence within reasonable time scales, providing mathematical rigor to the solutions.
- **Scalability:** It is essential to demonstrate scalability with increasingly large-scale power system benchmarks under diverse but realistic operational conditions.
- **Communication Efficiency:** Algorithms should require simple and limited communication that can be implemented using existing technologies and infrastructures.

The contributions of the paper are three-fold:

- 1) We propose a two-level distributed optimization algorithm for generic NLP with guaranteed convergence. The upper level employs barrier methods to handle inequality constraints, while the lower level uses ALADIN to solve the resulting smoothed equality-constrained problems. This improves scalability by avoiding combinatorial challenges [33, Ch. 15.2]. Additionally, by condensing the derivatives using the Schur complement, it reduces the overall computational and communication overhead, as well as the risks exposing topology information contained in the sparsity pattern of Jacobian and Hessian matrices.
- 2) We demonstrate the scalability of this algorithm through extensive large-scale simulations with different operation scenarios. Under the single program multiple data (SPMD) paradigm, the computational tasks are distributed and processed in parallel with distributed memory. These tests account for synchronization overhead and show that the proposed approach outperforms the state-of-the-art centralized nonlinear solver IPOPT [35] on modest hardware.
- 3) We conduct a systematic analysis of network decomposition and its influence on convergence, theoretical communication requirements, and practical performance of the proposed distributed algorithm. Alongside these findings, we discuss criteria for optimal network decompositions, distributed automatic differentiation (AD), and strategies to ensure resilience against single-point failures.

The rest of this paper is organized as follows: Section II describes the AC OPF problem and its distributed formu-

lation. Section III introduces the proposed algorithm with convergence analysis. Section IV provides practical considerations, including network decomposition, distributed AD, and resilience to single-point failures. Section V discusses the large-scale simulation results in detail, while Section VI examines communication efforts under both theoretical and practical scenarios. Finally, Section VII concludes the paper.

II. PROBLEM FORMULATION

This section introduces the standard AC optimal power flow (OPF) formulation. We then explore graph-based decomposition methods and demonstrate how these can be reformulated into a generic distributed approach with affine consensus constraints.

A. Preliminaries

Let us consider a power system $\mathcal{S} = (\mathcal{N}, \mathcal{L}, \mathcal{R})$, where \mathcal{N} represents the set of buses, \mathcal{L} the set of lines and \mathcal{R} the set of regions into which the network is partitioned. Let $n^{\mathcal{N}}$, $n^{\mathcal{L}}$, and $n^{\mathcal{R}}$ denote the number of buses, lines, and regions, respectively. In this context, the complex voltage at a bus can be expressed in rectangular coordinates, i.e.,

$$V_i = u_i + \mathbf{j}w_i,$$

where u_i and w_i are the real and imaginary parts of the complex voltage V_i , respectively, and $\mathbf{j} = \sqrt{-1}$ represents the imaginary. The variables p_i^g, q_i^g (resp. p_i^l, q_i^l) represent the real and reactive power produced by generators (resp. loads) at bus i . These variables are set to 0 if no generator (resp. load) is connected to a bus i . The real and imaginary parts of the complex nodal admittance matrix Y are represented by G and B . The optimization state vector x includes all the real and imaginary parts of complex voltage and active and reactive generator injections, i.e., $x = (u, w, p^g, q^g) \in \mathbb{R}^{4n^{\mathcal{N}}}$.

B. Conventional AC Optimal Power Flow

The AC optimal power flow (OPF) problem with the complex voltage in rectangular coordinates can be written as follows

$$\min_x \sum_{i \in \mathcal{N}} \{a_{i,2} (p_i^g)^2 + a_{i,1} p_i^g + a_{i,0}\} \quad (1a)$$

$$\text{s.t. } p_i^{\text{inj}}(w, u) = p_i^g - p_i^l, \quad \forall i \in \mathcal{N}, \quad (1b)$$

$$q_i^{\text{inj}}(w, u) = q_i^g - q_i^l, \quad \forall i \in \mathcal{N}, \quad (1c)$$

$$p_{ij}^2 + q_{ij}^2 \leq \bar{s}_{ij}^2, \quad \forall (i, j) \in \mathcal{L}, \quad (1d)$$

$$\underline{v}_i^2 \leq u_i^2 + w_i^2 \leq \bar{v}_i^2, \quad \forall i \in \mathcal{N}, \quad (1e)$$

$$\underline{p}_i^g \leq p_i^g \leq \bar{p}_i^g, \quad \forall i \in \mathcal{N}, \quad (1f)$$

$$\underline{q}_i^g \leq q_i^g \leq \bar{q}_i^g, \quad \forall i \in \mathcal{N}, \quad (1g)$$

with power injection at bus $i \in \mathcal{N}$,

$$p_i^{\text{inj}}(u, w) = \sum_{k \in \mathcal{N}} G_{ik}(u_i u_k + w_i w_k) + B_{ik}(w_i u_k - u_i w_k),$$

$$q_i^{\text{inj}}(u, w) = \sum_{k \in \mathcal{N}} G_{ik}(w_i u_k - u_i w_k) - B_{ik}(u_i u_k + w_i w_k),$$

and power flow in line $(i, j) \in \mathcal{L}$,

$$p_{ij} = G_{ij}(u_i^2 - u_i u_j + w_i^2 - w_i w_j) + B_{ij}(u_i w_j - w_i u_j),$$

$$q_{ij} = B_{ij}\{u_i(u_j - u_i) + w_i(w_j - w_i)\} + G_{ij}(u_i w_j - w_i u_j),$$

where $a_{i,2}$, $a_{i,1}$, and $a_{i,0}$ are the polynomial coefficients for the operation cost of power generations at bus i . The symbols

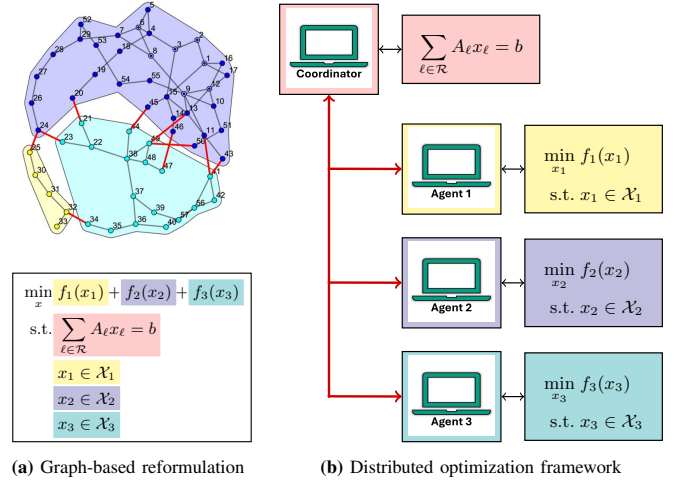


Fig. 1: Graph-based distributed optimization in power system applications

$\underline{\cdot}$ and $\bar{\cdot}$ denote upper and lower bounds for the respective state variables. Thus, problem (1) includes the active and reactive nodal power balances (1b)-(1c), apparent power limit on transmission lines (1d) and the bounds on the voltage magnitudes and power generations (1e)-(1g).

Remark 1 (Decomposition of OPF [36]). AC OPF problems (1) are well-suited for distributed approaches and parallel computing due to their repetitive nature across different components e.g. buses, lines, generators. This characteristic allows for easy decoupling of the objective and constraints and transformation into a standard distributed form.

C. Graph-Based Reformulation for Distributed Optimization

Regarding the distributed problem formulation, we share components with neighboring regions to ensure physical consistency, following [4]. For a given region $\ell \in \mathcal{R}$, buses entirely within the region form the core bus set $\mathcal{N}_\ell^{\text{core}}$, while those shared by neighboring regions are copy buses in $\mathcal{N}_\ell^{\text{copy}}$. Hence, the full bus set in region ℓ is given by $\mathcal{N}_\ell = \mathcal{N}_\ell^{\text{core}} \cup \mathcal{N}_\ell^{\text{copy}}$. Additionally, \mathcal{L}_ℓ represents the set of all transmission lines within region ℓ . This spatial decomposition, visualized in Fig. 1 using a partitioned IEEE 57-bus system, creates local subproblems while introducing shared variables at regional boundaries that require coordination.

The distributed reformulation process, illustrated in Fig. 1a, can transform a conventional AC OPF problem (1) into a distributed framework where:

- 1) each region ℓ solves a local subproblem with its own objective f_ℓ and feasible set \mathcal{X}_ℓ , and
- 2) a consensus mechanism enforces physical consistency across regions.

This yields the distributed formulation:

$$\min_x f(x) := \sum_{\ell \in \mathcal{R}} f_\ell(x_\ell) \quad (4a)$$

$$\text{s.t. } \sum_{\ell \in \mathcal{R}} A_\ell x_\ell = b \quad (4b)$$

$$c_\ell^E(x_\ell) = 0 \quad | \ell \in \mathcal{R} \quad (4c)$$

$$c_\ell^I(x_\ell) \leq 0 \quad | \ell \in \mathcal{R} \quad (4d)$$

where local state x_ℓ includes the voltage angle and magnitude θ_i, v_i for all buses $i \in \mathcal{N}_\ell$, and the generator injections p_i^g, q_i^g for all core buses $i \in \mathcal{N}_\ell^{\text{core}}$. In a specific region $\ell \in \mathcal{R}$, f_ℓ represents the local cost function concerning core generators in the region ℓ . Function c_ℓ^E encompasses the nodal power balance (1b)-(1b) for all core buses $i \in \mathcal{N}_\ell^{\text{core}}$, and c_ℓ^I collects system limits on voltage magnitude (1e), active and reactive power generation (1f)-(1g) for all core bus $i \in \mathcal{N}_\ell^{\text{core}}$, as well as power limit (1d) on the transmission lines $(i, j) \in \mathcal{L}_\ell$ within region ℓ . The consensus constraint (4b) ensures consistency of core and copy variables between neighboring regions.

As shown in Fig. 1b, this architecture enables parallel computation through regional agents that solve local subproblems, coordinated by a central mechanism enforcing consensus. This approach preserves physical consistency while improving scalability, as regional solutions only require coordination at shared boundaries rather than full system visibility.

III. DISTRIBUTED NONCONVEX OPTIMIZATION

A. Limitations of Standard ALADIN

Augmented Lagrangian-based Alternating Direction Inexact Newton method (ALADIN), first proposed in [31], was developed for generic nonconvex nonlinear programming (NLP) with guarantees for global convergence. Unlike the first-order ADMM, ALADIN integrates a sequential quadratic programming (SQP) framework. This involves using the active-set method and solving the equality-constrained quadratic program (QP) problems in the coordinator. This enable quadratic convergence rates and strong scalability for problems without inequality constraints [31], [32].

A key limitation arises when inequality constraints are present. Similar to traditional SQP approaches, the active-set method introduces combinatorial challenges [33, Ch. 15.2], as the number of possible active-sets increases exponentially with the number of inequalities. This scalability challenge of the standard ALADIN has been acknowledged in recent studies [16], [34]. It restricts prior studies on distributed AC OPF using ALADIN to systems with fewer than 1000 buses or a merged network with loosely inter-regional coupling, making the problem relatively easier to be solved.

Another limitation is communication overhead. The standard ALADIN requires derivative information from each subproblem to construct a second-order approximated model of the original problems (4) in the coordinator. While this accelerates convergence compared with first-order algorithms like ADMM, it significantly increases computational and communication demands. As system size grows, evaluating the second-order derivatives and coordinating communication between local agents and a central coordinator become significant bottlenecks. Previous research has focused mainly on the numerical performance of the ALADIN algorithm, with limited exploration of distributed implementations. This leaves the impact of communication overhead on practical performance unclear. Additionally, optimizing over networks, such as power systems, may reveal the network topology of the power networks through the sparsity pattern of local derivative information, raising privacy concerns.

In the present paper, we integrate smoothing techniques—proven effective for large-scale distributed convex optimization [37]—alongside Schur complement and distributed inertia correction. This improves scalability and reduces communication overhead while preserving convergence guarantees. The algorithm framework, convergence analysis, and criteria for optimal network decomposition are detailed in later sections.

B. Algorithm Framework

To solve the Problem (4), we employ a two-level framework. At the upper level, we adopt barrier methods to handle inequality constraints instead of relying on the active-set method. By using the barrier to smooth the inequalities, the original problem (4) is transformed into a series of equality-constrained barrier problems:

$$\min_{x, s} \quad f^\mu(x, s) = \sum_{\ell \in \mathcal{R}} f_\ell^\mu(x_\ell, s_\ell) \quad (5a)$$

$$\text{s.t.} \quad \sum_{\ell \in \mathcal{R}} A_\ell x_\ell = b \quad | \quad \lambda \quad (5b)$$

$$c_\ell^E(x_\ell) = 0 \quad | \quad \gamma_\ell, \ell \in \mathcal{R} \quad (5c)$$

$$c_\ell^I(x_\ell) + s_\ell = 0 \quad | \quad \kappa_\ell, \ell \in \mathcal{R} \quad (5d)$$

where the local barrier objective is:

$$f_\ell^\mu(x_\ell, s_\ell) = f_\ell(x_\ell) - \mu \sum_{m \in \mathcal{C}_\ell^I} \ln(s_\ell^{(m)}),$$

and $s_\ell \geq 0, \forall \ell \in \mathcal{R}$ is implicitly enforced because minimization with the barrier term prevents s_ℓ from approaching zero [33].

The corresponding KKT conditions of the barrier problems (5), the so-called *perturbed KKT conditions*, can be written as

$$\nabla f_\ell(x_\ell) + R_\ell^\top \kappa_\ell + J_\ell^\top \gamma_\ell + A_\ell^\top \lambda = 0, \quad \forall \ell \in \mathcal{R} \quad (6a)$$

$$-\mu \mathbf{1} + \mathcal{S}_\ell \kappa_\ell = 0, \quad \forall \ell \in \mathcal{R} \quad (6b)$$

$$c_\ell^E(x_\ell) = 0, \quad \forall \ell \in \mathcal{R} \quad (6c)$$

$$c_\ell^I(x_\ell) + s_\ell = 0, \quad \forall \ell \in \mathcal{R} \quad (6d)$$

$$\sum_{\ell \in \mathcal{R}} A_\ell x_\ell - b = 0 \quad (6e)$$

with $R_\ell = \nabla c_\ell^I(x_\ell)^\top$, $J_\ell = \nabla c_\ell^E(x_\ell)^\top$ and $\mathcal{S}_\ell = \text{diag}(s_\ell)$, where $\mathbf{1}$ denotes the vector of all ones with the respective dimension. Note that the conditions (6) for $\mu = 0$, together with $\kappa_\ell, s_\ell \geq 0, \forall \ell \in \mathcal{R}$, are equivalent to the KKT conditions for the original problem (4) [35].

Remark 2. The solution to the problem (5) is given by

$$x^*(\mu) = \arg \min_x \quad (5a), \text{ s.t. } (5b) - (5d).$$

As the barrier parameter μ approaches zero, the solution $x^*(\mu)$ converges to the solution of the original problem (4).

Then, in the lower level, ALADIN is used to solve a smoothed problem (5) for a fixed value of barrier parameter μ in a distributed manner. Once sufficient accuracy is achieved, the barrier parameter is decreased, and the process continues until the algorithm converges. **1) Decoupled Step.** The proposed distributed algorithm is outlined in Algorithm 1 in detail. Firstly, decoupled barrier NLP subproblems (7) are solved locally for each region $\ell \in \mathcal{R}$. After solving these local subproblems, the derivatives are evaluated and condensed locally at the local solution

Algorithm 1 Barrier ALADIN

Initialization:

Input: initial primal and dual points (z, λ) , positive penalty parameters ρ, μ and scaling symmetric matrices $\Sigma_\ell \succ 0$

Repeat:

- 1: Solve decoupled NLPs for all $\ell \in \mathcal{R}$ \triangleright Parallel

$$\min_{x_\ell, s_\ell} f_\ell^\mu(x_\ell, s_\ell) + \lambda^\top A_\ell x_\ell + \frac{\rho}{2} \|x_\ell - z_\ell\|_{\Sigma_\ell}^2 \quad (7a)$$

$$\text{s.t. } c_\ell^E(x_\ell) = 0 \quad | \gamma_\ell, \quad (7b)$$

$$c_\ell^I(x_\ell) + s_\ell = 0 \quad | \kappa_\ell, \quad (7c)$$

with $\kappa_\ell, s_\ell \geq 0$, and use initial guess for κ_ℓ, s_ℓ from (12) if available.

- 2: Evaluate E_ℓ^μ and E_ℓ^0 from (13), and condense derivatives for all $\ell \in \mathcal{R}$ \triangleright Parallel

$$W_\ell = -\bar{A}_\ell \bar{H}_\ell^{-1} \bar{A}_\ell^\top \quad (8a)$$

$$h_\ell = A_\ell x_\ell - \bar{A}_\ell \bar{H}_\ell^{-1} \bar{g}_\ell \quad (8b)$$

where $\bar{H}_\ell, \bar{g}_\ell$ and \bar{A}_ℓ are local curvature information at decoupled solution (x_ℓ, s_ℓ) ; more detailed description see (18)-(22).

- 3: Send $E_\ell^\mu, E_\ell^0, A_\ell x_\ell, W_\ell$ and h_ℓ to coordinator, and run Algorithm 2 to correct inertia if the inertia condition (25) is not satisfied \triangleright Synchronize

- 4: Terminate if condition (15) is satisfied. \triangleright Centralized

- 5: Update barrier parameter by (17) if condition (16) is satisfied. \triangleright

Centralized

- 6: Solve coordination problem \triangleright Centralized

$$W \Delta \lambda = -h \quad (9)$$

with $W = \sum_{\ell \in \mathcal{R}} W_\ell$

- 7: Send $\Delta \lambda$ back to each local agent \triangleright Synchronize

- 8: Recover local primal-dual step for all $\ell \in \mathcal{R}$ \triangleright Parallel

$$\begin{pmatrix} \Delta x_\ell \\ \Delta \gamma_\ell \end{pmatrix} = -\bar{H}_\ell^{-1} \bar{A}_\ell^\top \Delta \lambda - \bar{g}_\ell, \quad (10a)$$

$$\Delta s_\ell = -c_\ell^I(x_\ell) - s_\ell - R_\ell \Delta x_\ell, \quad (10b)$$

$$\Delta \kappa_\ell = -\kappa_\ell + S_\ell^{-1}(\mu \mathbf{1} - \mathcal{K}_\ell \Delta s_\ell), \quad (10c)$$

and obtain local primal-dual steplength $(\beta_\ell^p, \beta_\ell^d)$ by using the fraction-to-boundary method

$$\beta_\ell^p = \max\{\beta \in (0, 1] : s_\ell + \beta \Delta s_\ell \geq (1 - \tau) s_\ell\} \quad (11a)$$

$$\beta_\ell^d = \max\{\beta \in (0, 1] : \kappa_\ell + \beta \Delta \kappa_\ell \geq (1 - \tau) \kappa_\ell\}. \quad (11b)$$

- 9: Update primal-dual variables by \triangleright Synchronize

$$z_\ell^+ = z_\ell + \alpha_1(x_\ell - z_\ell) + \alpha_2 \beta^p \Delta x_\ell, \quad \forall \ell \in \mathcal{R} \quad (12a)$$

$$s_\ell^+ = s_\ell + \alpha_2 \beta^p \Delta s_\ell, \quad \forall \ell \in \mathcal{R} \quad (12b)$$

$$\kappa_\ell^+ = \kappa_\ell + \alpha_2 \beta^p \Delta \kappa_\ell, \quad \forall \ell \in \mathcal{R} \quad (12c)$$

$$\lambda^+ = \lambda + \alpha_3 \beta^d \Delta \lambda, \quad (12d)$$

with

$$\beta^p = \min_{\ell \in \mathcal{R}} \beta_\ell^p, \quad (12e)$$

where, $\alpha_1, \alpha_2, \alpha_3$ are determined by Algorithm 3. Alternatively, for full-step updates without globalization, set $\alpha_1 = \alpha_2 = \alpha_3 = 1$.

(x_ℓ, s_ℓ) using the Schur complement. These derivatives are later utilized in the next stages of the distributed optimization process to facilitate communication and coordination between regions. It is important to note that both Step 1 and Step 2 can be executed in parallel, enhancing the efficiency of the overall process.

Remark 3. When solving the decoupled NLP subproblems, the fraction-to-boundary method [33, Ch. 19.2] is essential to ensure that the dual variables κ_ℓ and the slack variables s_ℓ remain positive throughout the iteration. This is a critical requirement for the proper functioning of barrier-based approaches.

2) *Assessing Optimality Conditions* To assess the convergence of the inner ALADIN algorithm, we need to evaluate

the perturbed KKT conditions (6). After solving the decoupled barrier NLP subproblems (7), we first evaluate the decoupled optimality residual (6a)-(6d) locally, defined by:

$$E_\ell^\mu(x_\ell, s_\ell, \lambda, \kappa_\ell, \gamma_\ell) = \max \left\{ \frac{\|\nabla_x \mathcal{L}_\ell(x_\ell, \lambda, \kappa_\ell, \gamma_\ell)\|_\infty}{s_\ell^d}, \frac{\|S_\ell \kappa_\ell - \mu \mathbf{1}\|_\infty}{s_\ell^c}, \left\| \begin{bmatrix} c_\ell^E(x_\ell) \\ c_\ell^I(x_\ell) + s_\ell \end{bmatrix} \right\|_\infty \right\} \quad (13)$$

with scaling parameters $s_\ell^d, s_\ell^c \geq 1$.

Each region $\ell \in \mathcal{R}$ sends its local residual E_ℓ^μ and the coupling term $A_\ell x_\ell$ to the coordinator, which computes the global optimality residual as:

$$E^\mu(x, s, \lambda, \kappa, \gamma) = \max \left\{ \max_{\ell \in \mathcal{R}} \{E_\ell^\mu(x, s, \lambda, \kappa, \gamma)\}, \left\| \sum_{\ell \in \mathcal{R}} A_\ell x_\ell - b \right\|_\infty \right\}. \quad (14)$$

For the original problem (4), setting $\mu = 0$ gives the residual E^0 . When the current primal-dual iterate $(x, s, \lambda, \kappa, \gamma)$ satisfies:

$$E^0(x, s, \lambda, \kappa, \gamma) \leq \epsilon, \quad (15)$$

where ϵ is a user-defined tolerance, and the slack-dual variables (s_ℓ, κ_ℓ) remain positive at the decoupled solutions (see Remark 3), the solution also satisfies the KKT conditions of the original problem (4). Therefore, the algorithm terminates when condition (15) is met.

To achieve fast local convergence, we adopt the barrier update strategy outlined in [38, Strategy 2] [35], which guarantees superlinear convergence under the second order sufficient condition (SOSC). Let ν denote the iteration counter for the outer loop, and μ_ν the current barrier parameter. When the primal-dual iterates $(x, s, \lambda, \kappa, \gamma)$ of the barrier problem (5) satisfies the tolerance

$$E^{\mu_\nu}(x, s, \lambda, \kappa, \gamma) \leq \eta^- \mu_\nu, \quad (16)$$

for a constant $\eta^- > 0$. In our implementation, the tolerance parameter is set as $\eta^- = 10$. The barrier parameter is updated as follows:

$$\mu_{\nu+1} = \max \left\{ \frac{\epsilon}{10}, \min \left\{ \frac{\mu_\nu}{5}, \mu_\nu^{1.5} \right\} \right\} \quad (17)$$

This approach ensures that the barrier parameter decreases at a superlinear rate, thereby accelerating convergence.

3) *Condensed Coordination Step* The coordination problem (9) is one iteration of the second-order multiplier method [39]. Consider applying a Newton step to the primal-dual perturbed KKT conditions (6):

$$\begin{bmatrix} \nabla_{xx}^2 \mathcal{L} & 0 & J^\top & R^\top & A^\top \\ 0 & \mathcal{K} & 0 & S & 0 \\ J & 0 & 0 & 0 & 0 \\ R & I & 0 & 0 & 0 \\ A & 0 & 0 & 0 & 0 \end{bmatrix} \begin{bmatrix} \Delta x \\ \Delta s \\ \Delta \gamma \\ \Delta \kappa \\ \Delta \lambda \end{bmatrix} = \begin{bmatrix} -g \\ \mu \mathbf{1} - \mathcal{K} s \\ -c^E(x) \\ -c^I(x) - s \\ b - Ax \end{bmatrix}, \quad (18)$$

where the KKT matrix is asymmetric, to obtain this linear system. By eliminating the slack variables Δs and dual variables $\Delta \kappa$, we can obtain a symmetric linear system. This results in the following coupled system:

$$\begin{bmatrix} H & J^\top & A^\top \\ J & & \\ A & & \end{bmatrix} \begin{pmatrix} \Delta x \\ \Delta \gamma \\ \Delta \lambda \end{pmatrix} = - \begin{pmatrix} g \\ c^E(x) \\ Ax - b \end{pmatrix} \quad (19)$$

with

$$H = \text{blkdiag}(H_\ell), \quad H_\ell \approx \nabla_{xx} L_\ell + R_\ell^\top \mathcal{S}_\ell^{-1} \mathcal{K}_\ell R_\ell,$$

$$g = \text{vertcat}(g_\ell), \quad g_\ell = \nabla_x L_\ell + R_\ell^\top \mathcal{S}_\ell^{-1} (\mu \mathbf{1} + \mathcal{K}_\ell c_\ell^1(x_\ell)),$$

$$J = \text{blkdiag}(J_\ell), \quad A = \text{horzcat}(A_\ell).$$

The equivalent QP subproblem

$$\min_{\Delta x} \sum_{\ell \in \mathcal{R}} \left\{ \frac{1}{2} \Delta x_\ell^\top H_\ell \Delta x_\ell + g_\ell^\top \Delta x_\ell \right\} \quad (20a)$$

$$\text{s.t.} \quad \sum_{\ell \in \mathcal{R}} A_\ell \Delta x_\ell = b - Ax \quad | \quad \lambda + \Delta \lambda \quad (20b)$$

$$J_\ell \Delta x_\ell = -c_\ell^E(x_\ell), \quad \ell \in \mathcal{R}. \quad (20c)$$

is similar to the coupled QP step in the standard ALADIN [31, Alg. 2].

Next, we follow the Second-Order Multiplier method [40] to further condense (19) using the Schur complement. Reordering the elements in the Newton step (19), it can be rewritten as

$$\begin{bmatrix} \bar{H}_1 & & \bar{A}_1^\top \\ & \ddots & \vdots \\ & & \bar{H}_n & \bar{A}_n^\top \\ \bar{A}_1 & \dots & \bar{A}_n & 0 \end{bmatrix} \begin{pmatrix} \Delta \bar{x}_1 \\ \vdots \\ \Delta \bar{x}_n \\ \Delta \lambda \end{pmatrix} = - \begin{pmatrix} \bar{g}_1 \\ \vdots \\ \bar{g}_n \\ Ax - b \end{pmatrix} \quad (21)$$

with local primal-dual iterates $\Delta \bar{x}_\ell = (\Delta x_\ell^\top, \Delta \gamma_\ell^\top)^\top$ and curvature information

$$\bar{H}_\ell = \begin{bmatrix} H_\ell & J_\ell^\top \\ J_\ell & c_\ell^E(x_\ell) \end{bmatrix}, \quad \bar{g}_\ell = \begin{pmatrix} g_\ell \\ c_\ell^E(x_\ell) \end{pmatrix} \text{ and } \bar{A}_\ell = [A_\ell \quad 0] \quad (22)$$

or written in a compact form as an alternative:

$$\begin{bmatrix} \bar{H} & \bar{A}^\top \\ \bar{A} & 0 \end{bmatrix} \begin{pmatrix} \Delta \bar{x} \\ \Delta \lambda \end{pmatrix} = - \begin{pmatrix} \bar{g} \\ Ax - b \end{pmatrix} \quad (23)$$

with block diagonal matrix $\bar{H} = \text{blkdiag}(\bar{H}_\ell)$. By using the Schur complement, we have

$$W \Delta \lambda = -h$$

with

$$W = \sum_{\ell \in \mathcal{R}} W_\ell, \quad h = -b + \sum_{\ell \in \mathcal{R}} h_\ell,$$

where W_ℓ and h_ℓ can be computed in each agent ℓ in parallel

$$W_\ell = -\bar{A}_\ell \bar{H}_\ell^{-1} \bar{A}_\ell^\top \\ h_\ell = A_\ell x_\ell - \bar{A}_\ell \bar{H}_\ell^{-1} \bar{g}_\ell$$

Once the coordinator receives the dual Hessian W_ℓ and the dual gradient h_ℓ from all local agents $\ell \in \mathcal{R}$, and a descent direction can be guaranteed, then we solve the coordination problem in dual space (9); otherwise, Algorithm 2 is called to correct the inertia of the dual Hessian W , which is a symmetric matrix. Details about the criterion of descent direction and corresponding modification will be discussed in the following section.

Remark 4. The Schur complement method is particularly effective when 1) \bar{H}_ℓ is easy to invert or 2) the number of consensus constraints, denoted by N^λ , is small, which reduces the complexity of the matrix-matrix product $\bar{H}_\ell^{-1} \bar{A}_\ell^\top$.

Remark 5. Further condensing the KKT linear systems (19) serves to reduce the communication effort between agents and the coordinator, such that only the dual Hessian W_ℓ and the dual gradient g_ℓ need to be communicated. This not only reduces the data exchanged between agents and the coordinator but also distributes part of the coordinator's

computational tasks to the local agents. By allowing these tasks to be handled in parallel by the agents, the overall computational burden on the coordinator is reduced, leading to an improvement in the total computation time.

Once the coordination problem (9) is solved, the dual step $\Delta \lambda$ is sent back to the local agents, and the full primal-dual step can be recovered locally by (10):

$$\begin{pmatrix} \Delta x_\ell \\ \Delta \gamma_\ell \end{pmatrix} = -\bar{H}_\ell^{-1} \bar{A}_\ell^\top \Delta \lambda - \bar{g}_\ell, \\ \Delta s_\ell = -c_\ell^I(x_\ell) - s_\ell - R_\ell \Delta x_\ell, \\ \Delta \kappa_\ell = -\kappa_\ell + \mathcal{S}_\ell^{-1} (\mu \mathbf{1} - \mathcal{K}_\ell \Delta s_\ell),$$

Having recovered local variables in each agent, primal and dual steplengths $\beta_\ell^p, \beta_\ell^d \in (0, 1]$ are determined by fraction-to-the-boundary rule in each local agent $\ell \in \mathcal{R}$. By evaluating steplengths locally, no full step information is required during the coordination.

The primal-dual iterates are then updated according to (12), where the shortest primal step length (12e) is used. If a globalization strategy is required, the parameters $\alpha_1, \alpha_2, \alpha_3$ are set as defined by Algorithm 3. Alternatively, for full-step updates, set $\alpha_1 = \alpha_2 = \alpha_3 = 1$.

Additionally, the dual variables $(\gamma_\ell, \kappa_\ell)$ can be updated locally by

$$\begin{aligned} \kappa_\ell^+ &= \kappa_\ell + \alpha_2 \beta_\ell^d \Delta \kappa_\ell, & \forall \ell \in \mathcal{R} \\ \gamma_\ell^+ &= \gamma_\ell + \alpha_2 \beta_\ell^p \Delta \gamma_\ell, & \forall \ell \in \mathcal{R} \end{aligned}$$

These updates help refine the initial guess for the decoupled NLPs (7) in subsequent iterations with additional communication overhead.

C. Distributed Inertia Correction

Before we go into distributed Hessian regularization, we introduce the definition of inertia of a symmetric matrix:

Definition 1 (Inertia [41]). The inertia of a symmetric matrix K is the triple $\text{inertia}(K) = (n^+, n^-, n^0)$, where $n^+, n^-,$ and n^0 denote the number of positive, negative, and zero eigenvalues of K , respectively.

From [41], we know that the perturbed Newton-step (19) is a strict descent direction of the equivalent QP subproblems if

$$\text{inertia}(K) = (N^x, N^E + N^\lambda, 0) \quad (24)$$

with $N^x = \sum_{\ell \in \mathcal{R}} N_\ell^x$ and $N^E = \sum_{\ell \in \mathcal{R}} N_\ell^E$, where K denote the corresponding perturbed KKT matrix in (19). However, under the proposed distributed framework (Algorithm 1), it is hard to determine the inertia of the perturbed KKT matrix.

To extend the condition (24) to the condensed linear system (9), we rely on the following property of inertia:

Lemma 1 (Haynsworth inertia additivity formula [42], [43]). Given that

$$K = \begin{bmatrix} K_{11} & K_{21}^\top \\ K_{21} & K_{22} \end{bmatrix}$$

is a Hermitian matrix and let K_{11} be the nonsingular submatrix of K and let

$$\Lambda = K_{22} - K_{21} K_{11}^{-1} K_{21}^\top$$

be the Schur complement of K_{11} in K . Then

$$\text{inertia}(K) = \text{inertia}(K_{11}) + \text{inertia}(\Lambda).$$

This Lemma indicates the inertia change rule by using the Schur complement.

Theorem 1. Let $K \in \mathbb{R}^{(N^x + N^E + N^\lambda) \times (N^x + N^E + N^\lambda)}$ be the perturbed KKT matrix in (19), i.e.,

$$K = \begin{bmatrix} H & J^\top & A^\top \\ J & & \\ A & & \end{bmatrix}$$

and let the Jacobian $\bar{J} = [J^\top, A^\top]^\top$ be of full-row rank. Then, if dual Hessian W satisfies the inertia condition

$$\text{inertia}(W) = (N^x, N^E + N^\lambda, 0) - \sum_{\ell \in \mathcal{R}} \text{inertia}(\bar{H}_\ell), \quad (25)$$

H is positive definite on the nullspace of the Jacobian \bar{J} and the equivalent QP subproblem has a strict local minimizer.

Proof. As a direct result of Lemma 1, we have

$$\begin{aligned} \text{inertia}(K) &= \text{inertia}(W) + \text{inertia}(\bar{H}) \\ &\Downarrow \text{block diagonal structure of } \bar{H} \text{ in (21)} \\ &= \text{inertia}(W) + \sum_{\ell \in \mathcal{R}} \text{inertia}(\bar{H}_\ell). \end{aligned}$$

Then, the conclusion follows from condition (24). \square

Condition (25) can be viewed as a distributed variant of the conventional inertia condition (24), where the inertia of the local matrix \bar{H} can be evaluated in parallel by each agent when condensing the derivatives (8). Based on a centralized inertia correction framework in [35], we propose a distributed inertia correction algorithm to validate the inertia and modify the Hessian when necessary. The distributed inertia correction process is detailed in Algorithm 2, which operates under the assumption that the consensus matrix A is nonsingular. This assumption typically holds for distributed problems, and the problem can be reformulated if it does not.

Algorithm 2 Distributed inertia Correction

Input: δ_x^{last} , $\text{inertia}(W)$, $\text{inertia}(\bar{H})$, $\forall \ell \in \mathcal{R}$
1: **if** the inertia condition (25) is satisfied **then**
2: $\delta_x^{\text{last}} = 0$
3: **else**
4: **if** $\delta_x^{\text{last}} = 0$ **then**
5: $\eta^{\text{inc}} = \eta^{\text{fast}}$ and $\delta^x = \delta_0^x$
6: **else**
7: $\eta^{\text{inc}} = \eta^{\text{slow}}$ and $\delta^x = \max(\eta^{\text{red}} \delta_0^x, \bar{\delta}^x)$
8: **end if**
9: **if** $n^0 = 0$ **then**
10: $\delta^\gamma = 0$
11: **else**
12: $\delta^\gamma = \delta_0^\gamma$
13: **end if**
14: **while** the inertia condition (25) is not satisfied **do**
15: $\text{inertia}(\bar{H}_\ell) = \text{inertia} \left(\begin{bmatrix} H_\ell + \delta^x I & J_\ell^\top \\ J_\ell & -\delta^\gamma I \end{bmatrix} \right)$
16: $\text{inertia}(W) = \text{inertia} \left(-\sum_{\ell \in \mathcal{R}} \bar{A}_\ell \bar{H}_\ell^{-1} \bar{A}_\ell^\top \right)$
17: $\delta_x^{\text{last}} = \delta^x$
18: $\delta^x = \eta^{\text{inc}} \delta^x$
19: **end while**
20: **end if**
Return $\delta_x^{\text{last}} = \delta^x$

Algorithm 2 starts if the distributed inertia conditions (25) are not satisfied. If the inertia check fails, the regularization parameter δ^x is initialized based on the previous Newton step,

and progressively larger values of the regularization parameter δ^x are applied until the distributed inertia conditions (25) are met. This incremental adjustment ensures that the algorithm finds the smallest necessary perturbation to correct the inertia while maintaining the distributed structure of the optimization process.

Remark 6. Although the evaluation of the inertia of the local matrix \bar{H}_ℓ can be evaluated in parallel by local agents during the condensation of the derivatives (8), the condensation process itself is not computationally inexpensive. It is particularly expensive if the local agents are densely coupled and N^λ is relatively large, as noted in Remark 4. Furthermore, Algorithm 2 introduces additional iterative communication, which can further increase the overall computational overhead.

D. Convergence Analysis

Since the barrier subproblem is solved by an ALADIN-type algorithm, we need some basic assumptions to ensure its successful application.

Assumption 1. Local solutions of the barrier problems (5) with respect to barrier parameter $\mu \geq 0$ form a primal-dual central path $(x^*(\mu), \lambda^*(\mu), \kappa^*(\mu), \gamma^*(\mu))$ towards the solution of the original problem (4). At each point along this path, the following conditions hold:

- (a) For each region $\ell \in \mathcal{R}$, the local objective f_ℓ and constraint c_ℓ are twice differentiable in the neighbourhood of x_ℓ^* with Lipschitz continuous second derivatives.
- (b) The primal-dual points are regular [33] such that the linear independence constraint qualification (LICQ), strict complementarity conditions (SCC), and second order sufficient condition (SOSC) hold.

Now, we summarize the global convergence of the proposed Algorithm 1:

Theorem 2. Let Assumption 1 hold, let the penalty parameter ρ be sufficiently large such that

$$\nabla_{xx} L_\ell + R_\ell^\top \mathcal{S}_\ell^{-1} \mathcal{K}_\ell R_\ell + \rho \Sigma_\ell$$

is positive definite on the null space of J_ℓ for all $\ell \in \mathcal{R}$, and the line-search parameters $\alpha_1, \alpha_1, \alpha_1$ are determined by the globalization strategy [31, Alg. 3], then Algorithm 1 will terminate after a finite number of iterations.

Proof. The proof of Theorem 2 can be established in two steps. First, the barrier subproblem (5) with a fixed parameter μ is treated as a generic equality-constrained nonlinear programming (NLP) problem. By applying the ALADIN algorithm to solve these barrier problems, global convergence to $x^*(\mu)$ for each fixed barrier parameter μ can be established following [31, Sec. 7]. Second, the global convergence of the overall method to the solution x^* of the original problem (4) is achieved by monotonically decreasing the barrier parameter μ . As μ approaches zeros, $x^*(\mu)$ approaches the original solution x^* . \square

IV. PRACTICAL CONSIDERATIONS FOR IMPLEMENTATION

In this section, we discuss practical considerations for implementing the proposed Algorithm 1 within a distributed or

parallel computing environment. To illustrate the interactions in the distributed process, the process sequence of the proposed Algorithm 1 between the coordinator and local agents is depicted in Fig. 2. This figure emphasizes the flow of information and synchronization steps, visualizing the coordination for better understanding and practical deployment.

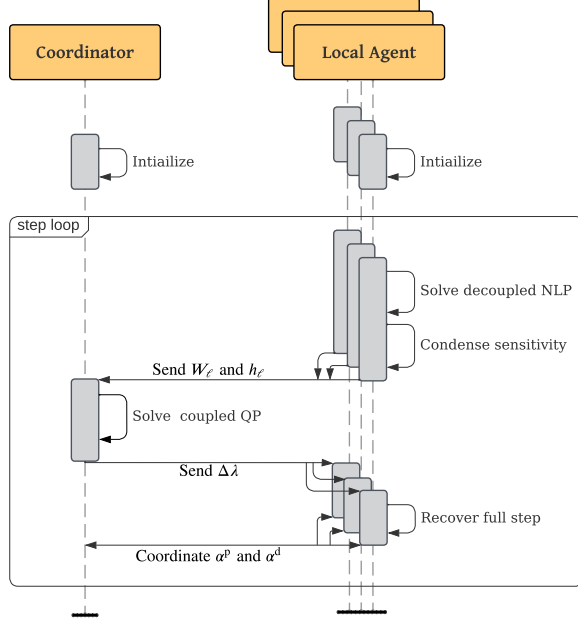


Fig. 2: Sequence diagram of the proposed Algorithm 1

To compare different networks and network decomposition, we define two measures:

- **Network Density:**

$$\zeta = \frac{N^{\text{line}}}{N^{\text{bus}}} \in \mathbb{R}_{++},$$

which indicates how densely buses are interconnected. This ratio does not depend on how the network is partitioned.

- **Coupling Density:**

$$\xi_\ell = \frac{N_\ell^{\text{cpl}}}{N_\ell^x} \in [0, 1],$$

where N_ℓ^{cpl} is the number of coupling variables, and N_ℓ^x is the total number of state variables in that region. The average coupling density across all regions is

$$\bar{\xi} = \frac{1}{N^{\text{reg}}} \sum_{\ell \in \mathcal{R}} \xi_\ell = \frac{1}{N^{\text{reg}}} \sum_{\ell \in \mathcal{R}} \frac{N_\ell^{\text{cpl}}}{N_\ell^x}.$$

Remark 7. For distributed optimization problems (4), N_ℓ^{cpl} equals the number of nonzero rows in A_ℓ . This indicates how many variables in the region ℓ are shared with neighboring regions.

A. Graph-based Decomposition

How the power grid is partitioned is essential for reducing problem complexity and improving parallelization. Traditional grid partitioning methods, such as those based on different system operators, hierarchical clustering, and electrical distances, do not adequately address the needs of distributed optimization and often fail to consider computational coupling, which strongly impacts the performance of distributed optimization methods, as observed by [18].

Recent advancements have introduced more sophisticated techniques. For instance, a spectral method, first proposed in [28], improves convergence using ADMM for large-scale problems [18]. However, the algorithm is initially designed for first-order methods and requires either *a priori knowledge* of the optimal operating point or *an assumption* of minimal deviation in power flow from this point.

By contrast, the proposed Algorithm 1 applies Newton-type methods, i.e., ALADIN, to solve the barrier problems (5), leveraging the Schur complement to condense second-order information. Two key factors improve efficiency in a distributed or parallel environment:

- **Equitable Partitioning:** As depicted in Fig. 1, the decoupled NLP subproblems (7) should be similar in size and computational effort. This prevents idle time and improves synchronization between local agents.
- **Reduced Coupling:** For a given network $\mathcal{S} = (\mathcal{N}, \mathcal{L}, \mathcal{R})$, a small coupling density $\xi_\ell \ll 1$ means fewer nonzero rows in both A_ℓ and \bar{A}_ℓ . This simplifies the computation of matrix products $\bar{H}_\ell^{-1} \bar{A}_\ell^\top$ during the derivative condensing step (8)—as discussed in Remark 4—and leads to smaller coupled QP subproblems (9). As a result, both communication and computation demands are reduced.

As demonstrated later in Section V-B, the condensation process and coupled coordination consume significant time for large-scale problems. Therefore, minimizing coupling has a more pronounced impact on the efficiency of the proposed Algorithm 1.

Recent research [44], [45] shows that the spectral method is outperformed by the Karlsruhe Fast Flow Partitioner (KaFFPa) from the Karlsruhe High Quality Partitioning (KaHIP) [46] when solving AC OPF for small- to medium-size systems using ALADIN. Unlike requiring prior knowledge or assumptions about the operating state, KaFFPa requires only a simple graph of the power system $(\mathcal{N}, \mathcal{L})$ and produces partitions of equal size with minimal connecting lines.

These two features—fewer connections and balanced partition sizes—align well with the abovementioned criteria. Therefore, the present paper adopts KaFFPa for grid partitioning. For a comprehensive description of the KaFFPa algorithm, we refer to [46], [47].

B. Distributed Automatic Differentiation

To run optimization algorithms in parallel, some earlier works [48], [49] indicate that running an optimization algorithm fully in parallel generally requires parallelizing the function evaluations, including evaluating derivatives in parallel. The challenge is to evaluate the derivatives while minimizing the communication between the different processes. This has led to the development of different prototypes for the Message Passing Interface (MPI) based parallel modelers [50]–[52]. Other research adopted approaches mainly from machine learning, using fast automatic differentiation (AD) libraries to efficiently generate derivatives on hardware accelerators such as Graphics Processing Units (GPUs) [53]–[56].

Unlike state-of-the-art parallel optimization methods, the proposed distributed algorithm for solving NLPs, e.g. AC OPFs, partitions the problem at the network level. Therefore,

neither the decoupled NLPs (7) nor the condensing steps (8) require global information from neighboring regions, allowing each local agent $\ell \in \mathcal{R}$ to evaluate the objective function f_ℓ and constraints c_ℓ independently in parallel. This reduces the complexity of communication and coordination using AD, making the parallel execution of the proposed distributed algorithm more straightforward.

C. Resiliency Against Single-Point Failures

The proposed distributed algorithm offers resiliency against single-point failures. As shown in the sequence diagram in Fig. 2, each local agent operates independently during the decoupled step for solving NLP subproblems and condensing sensitivities. If a single local agent fails, the remaining agents can continue operating, and the centralized coordinator can proceed with a reduced dataset.

Additionally, if the centralized coordinator fails, one local agent can take over the coordination tasks. This would not significantly reduce computation efficiency since local agents are idle during coordination. Moreover, this does not compromise data privacy since both the dual Hessian W_ℓ and the dual gradient g_ℓ are condensed and data-preserving.

Therefore, the proposed distributed algorithm ensures that failures do not lead to catastrophic breakdowns but instead allow for a degraded yet functional solution. By maintaining a distributed operational framework and relying on local computations, the system mitigates the risk associated with any single point of failure, thereby enhancing overall stability and reliability.

V. NUMERICAL TEST

This section demonstrates the performance of Algorithm 1 in solving large-scale AC optimal power flow (OPF) problems under different operating scenarios in a distributed computing environment. We assess the impact of coupling density and validate that this approach outperforms the state-of-the-art centralized nonlinear solver IPOPT [35].

A. Configuration and Setup

The framework is built on MATLAB-R2023b. The test cases are the largest test cases from the PGLib-OPF benchmark¹ [30] with version 23.07 and the large-scale test cases from [57]. The grid is partitioned into a different number of regions by using the KaFFPa algorithm from the KaHIP project [46]. The case studies are carried out on a small workstation with two AMD[®] Epyc 7402 24-core processors, i.e., 48 physical cores in total, and 128 GB installed RAM. The CasADi toolbox [58] is used in MATLAB. MA57 [59] is used as the linear solver. The centralized reference solution is obtained by solving the AC OPF problems with IPOPT [35].

To evaluate the performance of the proposed algorithm with minimal communication effort considered, we utilize the single program multiple data (SPMD) paradigm from the MATLAB parallel computing toolbox. This approach facilitates distributed computation by dividing work and data among agents

without shared memory. Communication between agents is managed using explicit MPI-style commands, taking into account the potential delays and synchronization requirements. In our setup, one worker functions as the coordinator while the others serve as local agents.

B. Impact of Network Decomposition

We analyze how the network decomposition affects performance by using three large power system test cases—case13659, case24464 and case7848—from the PGLib-OPF benchmark [30] and one additional large test case—case193k—from [57]. Table III shows detailed results for case78484 and case193k. In general, changes in the number of partitions have a larger effect on overall computing time rather than on the number of iterations required for convergence.

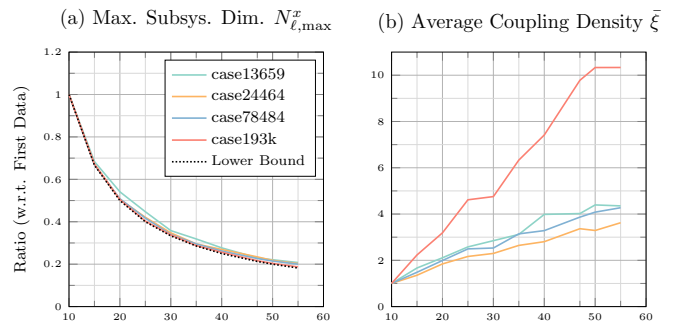


Fig. 3: Comparison of Network Decomposition on different power systems, i.e., case13659 from Pan European Grid Advanced Simulation and State Estimation (PEGASE) [60] [61], case24464 from ARPA-E grid optimization competition [62], case78484 from the US Eastern Interconnection states [63] and case193k from [57].

As illustrated in Fig. 3, for a given network, when we increase the number of partitions $|\mathcal{R}|$, each local subproblem becomes smaller, but the average coupling density $\bar{\xi}$ increases. In all four cases, the maximum subproblem size $N_{\ell, \max}^x$ is close to its theoretical lower bound, indicating that the KaFFPa balances the subsystems effectively.

A key difference is how the average coupling density $\bar{\xi}$ changes. In case193k, $\bar{\xi}$ grows faster than in the other three networks. This may be due to the network's topology: unlike the three PGLib-OPF cases with network density $\zeta \approx 1.5$, case193k has a lower network density ($\zeta = 1.186$). When partitioned into 10 regions, case193k shows an order-of-magnitude lower connectivity than case7848, experiencing faster increases in coupling density $\bar{\xi}$ than those with a dense network.

Fig 4 and Fig. 5 show how the average wall time per iteration is divided among local agents, the coordinator, and synchronization tasks, including communication overhead. Note that the sudden but simultaneous increases in coordinator (Fig. 4(b)) and synchronization overhead (Fig. 4(d)) stem from the additional inertia correction (Algorithm 2), which dampens the total wall time. Except for that inertia correction, when the partition number is less or equal to 47—corresponding to one local agent per core—a higher number of partitions distributes workload to more local agents and shortens their individual computation times. However, having more partitions

¹The PGLib-OPF is built for benchmarking AC OPF algorithms under IEEE PES Task Force. The benchmark is available on GitHub: <https://github.com/power-grid-lib/pglib-opf> and the baseline results for v23.07 can be found here: <https://github.com/power-grid-lib/pglib-opf/blob/master/BASELINE.md>

TABLE III: Comparing Different Region Numbers

Case	N^{bus}	N^{gen}	N^{line}	ζ	Partition Configuration					Iter	Init.	Convergence Performance (Wall Time [s])					
					$ \mathcal{R} $	$\bar{\xi}$	N^{conn}	N^λ	$N_{\ell, \max}^x$			dec.	cond.	coord.	rec.	syn.	total
case78484	78.8k	6.8k	126.1k	1.607	10	1.65%	395	1432	18062	80	48.40	17.20	188.39	9.27	11.96	4.93	231.75
					15	2.45%	587	2110	12070	78	31.64	9.86	99.90	11.36	7.46	6.06	134.64
					20	3.28%	777	2852	9184	90	24.73	10.65	80.50	22.47	7.75	9.54	130.90
					25	4.11%	990	3600	7530	76	18.70	7.20	81.11	24.88	6.98	11.70	131.88
					30	4.17%	1002	3642	6146	87	15.99	15.54	66.08	23.45	6.17	9.92	121.16
					35	5.18%	1241	4548	5334	76	12.13	6.44	53.23	28.80	5.58	10.75	104.80
					40	5.41%	1299	4756	4734	75	12.70	6.29	37.07	26.20	3.60	10.75	83.90
					47	6.37%	1532	5632	4092	76	11.91	5.73	32.77	32.94	3.35	10.93	85.73
					50	6.73%	1624	5950	3878	79	10.69	8.60	40.06	38.16	4.90	12.25	103.97
					55	7.04%	1690	6232	3614	79	12.12	10.53	59.62	37.92	7.11	13.94	129.12
case193k	192.7k	24.6k	228.6k	1.186	10	0.10%	55	220	44610	48	49.22	24.05	25.10	0.19	0.42	0.63	50.40
					15	0.22%	128	492	29972	46	34.08	13.32	23.60	0.27	0.58	0.58	38.34
					20	0.32%	179	702	22514	46	26.72	10.45	23.02	0.56	0.56	0.81	35.40
					25	0.46%	257	1004	17986	34	22.14	7.82	14.07	0.37	0.42	0.67	23.35
					30	0.47%	272	1050	15072	35	18.72	7.25	15.13	0.83	0.45	8.80	32.45
					35	0.63%	351	1368	12830	44	16.85	16.27	14.00	0.68	0.64	2.58	34.17
					40	0.74%	414	1612	11424	49	15.28	11.86	21.81	0.89	1.24	6.28	42.08
					47	0.97%	549	2138	9656	50	15.66	20.21	34.31	1.54	2.07	10.46	68.59
					50	1.03%	575	2252	9086	48	16.05	22.13	30.38	1.72	1.71	1.71	57.66
					55	1.03%	585	2278	8350	47	19.01	19.02	21.44	1.81	1.09	6.51	49.87

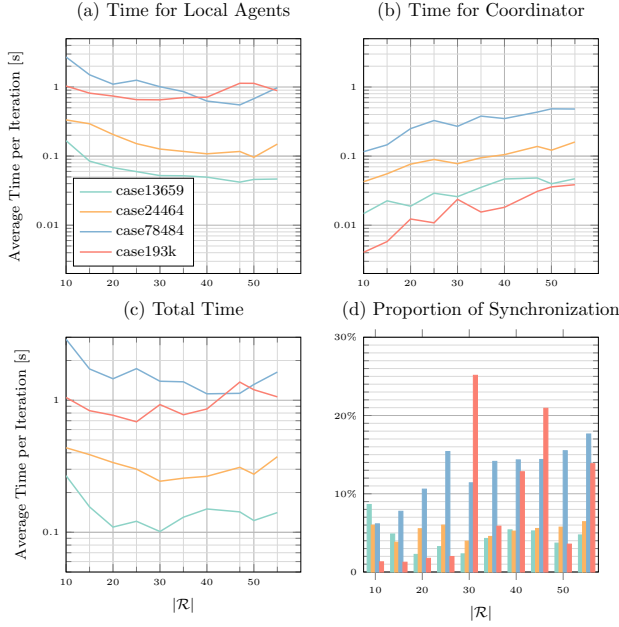


Fig. 4: Comparison of network decomposition on performance of the proposed Algorithm 1 on large-scale benchmarks.

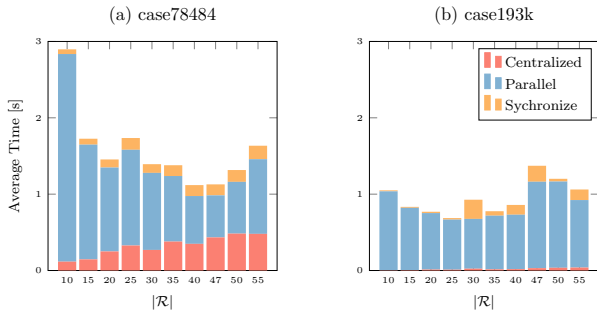


Fig. 5: Comparison of average wall times per iteration with different partition numbers for case78484 and case193k. Note that the parallel step encompasses the decoupled NLPs, condensing, and recovery steps.

also makes it more expensive to condense the derivatives (8) and enlarge the coordination problems (9), leading to higher total wall times.

Remark 8. For a given network, increasing the partition number $|\mathcal{R}|$ reduces the size of each subproblem and thus lowers each local agent's computation effort. However, it also raises the coupling density ξ_ℓ in each subproblem, making the local derivative condensing—especially computing $\bar{H}_\ell^{-1} \bar{A}_\ell^\top$ in (8a)—more expensive, and it also increases the size of the coupled QP subproblems (9) at the coordinator. Hence, when hardware resources are not limited, one must balance these trade-offs to find an optimal number of partitions.

The trade-off is also observed in Fig. 4: for the sparser network (case193k), where 25 partitions yield the shortest total time; beyond that, the total time grows. Although theoretically, partitioning the network can reduce further certain computational burdens, real-world performance depends on how local tasks, network density, and coordination overhead interact. More research and testing are needed to determine the best partitioning strategy in practice.

C. Centralized vs. Distributed

This section evaluates the performance of the proposed distributed approach against the state-of-the-art centralized nonlinear solver, IPOPT [35]. Both centralized and distributed setups utilize MA57 [59] as linear solver and CasADi [58] as automatic differentiation (AD) tools to ensure a fair comparison. Both use parallelization on the same hardware. The evaluation involves the largest test cases from the PGLib-OPF benchmark [30], each with three operation modes: standard (STD), active power increased (API) and small angle difference (SAD). Additionally, the four largest test cases from recent studies [57] are included. All these power grids are divided into 40 regions for analysis.

Detailed results in Table IV show that all the proposed distributed approaches converge to local optimizers. The optimality gaps between the centralized and distributed approaches are minimal, typically from 10^{-5} to 10^{-7} . Notably, the case78484,

with increased active power (API) using the centralized approach fails to converge, underscoring a potential scalability advantage of distributed approaches. Figure 6 compares

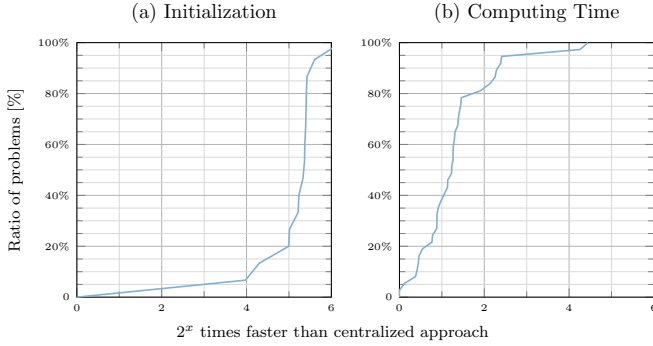


Fig. 6: Performance profile comparing the proposed Algorithm 1 with IPOPT on large-scale AC OPF benchmarks

the performance efficiency across all these large-scale test cases. The distributed implementation of AD, leveraging the SPMD model, significantly enhances the initialization speed. As shown in Fig. 6 (a), initialization is at least 16 times faster in more than 90% of the cases compared to the centralized approach. Regarding algorithm efficiency, the distributed algorithm is at least twice as fast as the centralized method in over 60% of the cases, with around 20% of cases achieving at least four times the speed, as shown in Fig. 6 (b). It suggests that the larger the test case, the greater the computational benefits offered by the distributed approach, highlighting its significant advantages for handling large-scale problems.

VI. ITERATIVE COMMUNICATION ANALYSIS

This section outlines the communication requirements for the proposed Algorithm 1. Building on our earlier work [23], we extend the theoretical analysis of ADMM and ALADIN from AC OPF problems to more general NLP formulations. We also evaluate practical performance using the large-scale benchmarks described in the previous section.

A. Worst-Case Communication Effort

Under worst-case scenarios, we assume that

- 1) The number of active constraints is equal to the number of state variables N_ℓ^x for each region $\ell \in \mathcal{R}$ such that LICQ still holds,
- 2) All matrices are dense, i.e., sparsity patterns are not considered, and
- 3) Only the full step is considered; neither the inertia correction (Algorithm 2) nor the globalization strategy, which requires additional communication, are covered in this analysis.

These assumptions enable a fair comparison of the three distributed algorithms, independent of problem-specific features such as sparsity patterns and complexity, while the practical evaluation is based on the four large-scale AC OPF benchmarks introduced in Section V.

For the proposed distributed Algorithm 1, the coordinator solves the condensed QP subproblem (9) with $W = \sum_{\ell \in \mathcal{R}} W_\ell$ and $h = -b + \sum_{\ell \in \mathcal{R}} h_\ell$. The communication effort for this is primarily associated with transferring the dual Hessian W_ℓ

and the dual gradient g_ℓ . Note that the coordinator is also responsible for reducing the barrier parameter μ (Step 5) before solving the condensed QP. Since h_ℓ can be viewed as linear mapping of μ , i.e., $h_\ell = h_{\ell,0} + \mu h_{\ell,\mu}$, the communication effort on h_ℓ would be doubled. Similar to the discussion earlier in this section, only N_ℓ^{cpl} elements from h_ℓ should be transferred to a centralized coordinator.

As a result, the forward communication in terms of floating-point numbers includes

$$\sum_{\ell \in \mathcal{R}} \underbrace{2N_\ell^{\text{cpl}}}_{h_\ell} + \underbrace{\frac{N_\ell^{\text{cpl}}(N_\ell^{\text{cpl}} + 1)}{2}}_{W_\ell}.$$

Once the condensed linear system (9) is solved, the proposed algorithm only requires the dual step $\Delta\lambda$ to be communicated during the backward phase, along with additional data for synchronizing the primal-dual steplength:

$$\underbrace{N_\ell^{\text{reg}}}_{\text{Eq. (12e)}} + \sum_{\ell \in \mathcal{R}} \underbrace{N_\ell^{\text{cpl}}}_{\Delta\lambda}.$$

B. Theoretical and Practical Comparison

Recall that $\xi_\ell = \frac{N_\ell^{\text{cpl}}}{N_\ell^x}$ measures the fraction of coupling variables in region $\ell \in \mathcal{R}$, while $\bar{\xi} = \sum_{\ell \in \mathcal{R}} \frac{\xi_\ell}{N_\ell^{\text{reg}}}$ is the average coupling density across all regions.

In many real-world scenarios, the number of regions N_ℓ^{reg} is much smaller than the total number of state variables $\sum_{\ell \in \mathcal{R}} N_\ell^x$, i.e.,

$$N_\ell^{\text{reg}} \ll \sum_{\ell \in \mathcal{R}} N_\ell^x.$$

Under this condition, the proposed algorithm demonstrates a significant reduction in communication effort compared to standard ALADIN, even in tightly coupled systems.

In practical optimization problems, the Hessian H and the Jacobian J are often sparse matrices. Therefore, assuming that all matrices are dense makes theoretical analysis easier but does not provide a fair comparison for standard ALADIN, which solves a full-dimensional coupled QP subproblem in this form (19).

To provide a fairer comparison, we conduct large-scale tests on AC OPF problems that reflect real-world conditions. We measure communication demands in single-precision floats and summarize the results in Table V.

Except for the final test case, the communication effort scales linearly for ADMM and quadratically for ALADIN as system size increases. In contrast, the proposed BALADIN exhibits intermediate scaling behavior. Additionally, BALADIN communication efficiency is significantly influenced by the overall coupling density $\bar{\xi}$ and can outperform ADMM in scenarios where each subproblem is more loosely coupled.

The newly proposed distributed optimization algorithm reduces communication efforts compared to standard ALADIN and can even match ADMM under certain conditions. The communication effort and the total computational time demonstrated in Section V depend partly on how the problem is decomposed and coupled.

TABLE IV: Benchmark

Case	N^x	N^c	ζ	$\bar{\xi}$	Mode	Convergence Performance (Wall Time [s])								Solution Quality			
						BALADIN				IPOPT				BALADIN		IPOPT	
						Iter	local	coord.	total	Iter	deriv.	lin.	total	Objective	Violation	Objective	Violation
case9241	21.4k	75.9k	1.7367	15.91%	STD	55	2.92	1.55	6.22	62	4.28	4.91	<i>10.68</i>	6243150	1.5E-08	6243090	3.9E-07
					API	49	1.61	1.77	5.09	101	7.27	9.97	<i>19.11</i>	7011200	4.5E-05	7011144	3.1E-07
					SAD	63	2.32	2.45	7.07	75	5.51	6.83	<i>13.94</i>	6318469	6.5E-06	6318469	3.9E-07
case9591	19.9k	76.5k	1.6594	26.01%	STD	46	1.71	4.54	8.36	52	3.60	10.48	<i>15.76</i>	1061684	1.3E-07	1061684	9.7E-08
					API	56	2.19	5.92	11.54	103	7.14	20.74	<i>29.96</i>	1570274	9.12E-05	1570264	2.2E-07
					SAD	57	2.18	4.90	9.64	81	5.60	15.78	<i>23.25</i>	1167400	4.43E-06	1167401	9.9E-08
case10000	24k	69.6k	1.3193	16.10%	STD	59	1.91	2.66	6.08	78	4.62	6.65	<i>12.69</i>	1354031	8.7E-09	1354031	5.1E-07
					API	61	1.88	2.79	6.23	85	5.04	7.21	<i>13.71</i>	2678660	4.5E-07	2678659	1.1E-07
					SAD	62	1.81	2.86	6.17	93	5.57	9.39	<i>16.44</i>	1490210	1.8E-07	1490210	4.8E-07
case10192	21.8k	81.6k	1.6695	23.68%	STD	70	3.53	6.56	13.37	50	4.05	8.84	<i>14.51</i>	1686923	4.7E-06	1686923	1.3E-07
					API	57	2.36	5.40	10.62	74	5.32	12.56	<i>19.61</i>	1977706	1.8E-05	1977686	2.5E-07
					SAD	57	2.44	5.12	10.09	66	5.28	11.57	<i>18.63</i>	1720194	3.9E-07	1720194	1.3E-07
case10480	22.5k	87.1k	1.7709	26.33%	STD	67	3.87	8.22	16.21	63	5.24	14.77	<i>22.09</i>	2314648	2.6E-06	2375951	1.1E-07
					API	65	3.58	9.38	17.41	66	5.17	15.46	<i>22.66</i>	2863484	1.9E-07	2924781	3.2E-07
					SAD	66	3.90	8.50	16.73	64	5.25	15.05	<i>22.35</i>	2314712	7.0E-07	2375951	1.1E-07
case13659	35.5k	102.4k	1.4984	9.65%	STD	57	2.50	2.65	8.65	180	15.96	26.80	<i>45.94</i>	8948202	7.5E-05	8948049	1.9E-07
					API	72	3.99	3.12	10.03	94	8.34	12.97	<i>23.57</i>	9385712	9.4E-05	9385711	2.5E-07
					SAD	62	2.74	2.49	7.88	302	26.81	118.70	<i>150.55</i>	9042199	1.2E-05	9042198	3.2E-07
case19402	40.7k	162.3k	1.7887	19.48%	STD	43	4.67	9.06	17.66	69	10.28	33.83	<i>48.14</i>	1977815	1.6E-06	1977815	1.2E-07
					API	64	6.73	15.62	28.72	69	10.32	34.53	<i>48.86</i>	2583662	1.2E-07	2583663	4.9E-07
					SAD	56	5.87	11.31	21.93	78	11.73	37.99	<i>53.92</i>	1983808	6.7E-06	1983809	1.2E-07
case20758	45.9k	162.3k	1.6063	13.35%	STD	73	6.99	10.62	24.79	43	6.17	12.55	21.69	2618662	3.1E-05	2618636	1.4E-07
					API	63	5.45	7.65	17.48	69	9.84	18.90	<i>32.15</i>	3126508	5.8E-05	3126508	1.6E-07
					SAD	70	5.91	7.44	18.20	55	7.83	15.50	<i>26.48</i>	2638220	4.1E-06	2638220	1.4E-07
case24464	52.1k	186.7	1.5458	11.97%	STD	53	5.60	4.97	13.05	57	9.48	21.04	<i>34.17</i>	2629531	2.1E-05	2629531	6.9E-08
					API	57	7.86	5.66	17.04	75	13.53	29.24	<i>46.90</i>	2684051	2.8E-05	2683962	3.2E-07
					SAD	64	6.39	7.22	18.60	68	11.40	25.56	<i>40.83</i>	2653958	9.9E-06	2653958	7.1E-08
case30000	67.1k	196.2k	1.1798	8.36%	STD	103	10.95	8.68	27.05	128	20.85	37.79	<i>63.38</i>	1142458	1.6E-05	1142331	4.6E-07
					API	100	11.91	10.13	30.80	147	23.67	45.18	<i>73.96</i>	1778059	4.5E-05	1777931	1.8E-07
					SAD	212	21.97	29.77	91.59	221	36.44	83.31	<i>126.23</i>	1317386	1.3E-05	1309979	2.0E-07
case78484	170.5k	613.5k	1.6057	6.37%	STD	75	47.63	22.74	80.35	95	52.10	131.07	<i>199.05</i>	15316174	2.1E-05	15315886	1.3E-07
					API	74	47.21	23.22	83.01	217	109.66	1688.24	<i>1808.58</i>	16140687	3.3E-07	19379770	1.3E+01
					SAD	77	49.79	24.17	83.92	96	53.68	132.43	<i>201.55</i>	15316174	1.7E-06	15315886	1.3E-07
case21k	47.6k	113.2k	1.1858	8.41%	STD	29	1.70	1.00	3.30	63	5.90	8.22	<i>16.08</i>	2592246	8.4E-06	2592098	1.2E-07
case42k	95.1k	226.5k	1.1858	4.94%	STD	42	5.14	1.39	7.80	66	12.55	17.53	<i>34.08</i>	2592459	2.2E-06	2592458	5.8E-07
case99k	224.2k	522.9k	1.1858	2.11%	STD	45	15.18	0.60	16.54	67	30.06	46.45	<i>86.50</i>	2594077	2.2E-06	2594077	5.6E-08
case194k	434.8k	1035.5k	1.1857	0.97%	STD	46	31.31	0.69	37.35	71	63.30	93.94	<i>178.33</i>	2595600	8.0E-07	2595599	4.1E-08

There are three configurations for test cases from PGLib-OPF: Standard (STD), representing nominal operating conditions; Active Power Increase (API), simulating heavily loaded scenarios; and Small Angle Difference (SAD), enforcing strict bounds on voltage phase angle difference.

TABLE V: Theoretical & Practical Iterative Communication Effort

	$\bar{\xi}$	ADMM	ALADIN	BALADIN
Forward	$\sum_{\ell \in \mathcal{R}} \frac{\xi_\ell}{N^{\text{reg}}}$	$\sum_{\ell \in \mathcal{R}} 2N_\ell^x$	$\sum_{\ell \in \mathcal{R}} (N_\ell^x)^2 + \frac{3 + 2\xi_\ell}{2} N_\ell^x$	$\sum_{\ell \in \mathcal{R}} \frac{\xi_\ell^2}{2} (N_\ell^x)^2 + \frac{5\xi_\ell}{2} N_\ell^x$
Backward	$\sum_{\ell \in \mathcal{R}} \frac{\xi_\ell}{N^{\text{reg}}}$	$\sum_{\ell \in \mathcal{R}} N_\ell^x$	$\sum_{\ell \in \mathcal{R}} (1 + \xi_\ell) N_\ell^x$	$2N^{\text{reg}} + \sum_{\ell \in \mathcal{R}} \xi_\ell N_\ell^x$
Total	$\sum_{\ell \in \mathcal{R}} \frac{\xi_\ell}{N^{\text{reg}}}$	$\sum_{\ell \in \mathcal{R}} 3N_\ell^x$	$\sum_{\ell \in \mathcal{R}} (N_\ell^x)^2 + \frac{5 + 4\xi_\ell}{2} N_\ell^x$	$2N^{\text{reg}} + \sum_{\ell \in \mathcal{R}} \frac{\xi_\ell^2}{2} (N_\ell^x)^2 + \frac{7\xi_\ell}{2} N_\ell^x$
case13659	9.64%	0.427 MB	2.388 MB	0.682 MB
case24464	11.97%	0.635 MB	4.276 MB	2.104 MB
case78484	6.37%	2.016 MB	13.731 MB	5.791 MB
case194k	0.97%	4.999 MB	20.226 MB	0.888 MB

Note: Theoretical worst-case communication efforts are expressed in terms of floating-point numbers, while practical communication efforts for large-scale AC OPF benchmarks are measured in MegaBytes, assuming the use of single-precision floating-point

VII. CONCLUSION & OUTLOOK

The present paper introduces a distributed approach for large-scale AC OPF problems with convergence guarantees and a rapid convergence rate. This approach enhances efficiency and scalability while preserving privacy by dividing extensive computational tasks into smaller with the Schur complement, parallelized operations. It can also be applied to other optimization and control problems in power system operations, as these problems involve repetitive expressions for each component type. Extensive simulations, based on the largest test cases under various operation scenarios, are used for the analysis of the impact of coupling density as well as to demonstrate that its performance surpasses the state-of-art centralized nonlinear solvers IPOPT [35] on moderate hardware.

While the current study presents a particularly favorable algorithm for distributed optimization in power systems, further research is essential to fully realize the potential of the proposed distributed approach. As noted in [31], [64], distributed implementations of globalization routines (e.g., line-search) remain challenging. Future directions include refining globalization techniques, reducing communication overhead, leveraging high-performance computing (HPC) platforms, and developing asynchronous variants for greater flexibility. Additionally, we plan to release an open-source MATLAB toolbox for the proposed approach, making it accessible for rapid prototyping and further research.

APPENDIX A

GLOBALIZATION STRATEGY

Algorithm 3 Globalization Strategy [31, Alg. 3] for the barrier problems (5)

Initialization: set $\alpha_1 = \alpha_2 = \alpha_3 = 1$.

a) If the iterates from Step 9 in Algorithm 1 satisfies

$$\Phi(z) - \Phi(x^+) \geq \eta \left(\sum_{i=1}^N \frac{\rho}{2} \|x_\ell - z_\ell\|_{\Sigma_\ell}^2 + \bar{\lambda} \left\| \sum_{i=1}^N A_\ell x_\ell - b \right\|_1 \right), \quad (26)$$

with $x^+ = x + \Delta x$, then return $\alpha_1 = \alpha_2 = \alpha_3 = 1$.

b) If the full step is not accepted, set $x^+ = x$ and $\lambda^+ = \lambda$. If inequality (26) holds, return $\alpha_1 = 1$ and $\alpha_2 = \alpha_3 = 0$.

c) If both a) and b) failed, set $x^+ = z$ and choose $\alpha_3 \in (0, 1]$ by solving

$$\alpha_3^* = \arg \max_{\alpha_3 \in (0, 1]} V_\rho(z, \lambda + \alpha_3(\lambda^{\text{QP}} - \lambda)) \quad (27)$$

with the objective function defined by a parametric optimization problem

$$V_\rho(\bar{x}, \lambda) = \min_x \sum_{i=1}^N \left\{ f_\ell(x_\ell) + \lambda^\top A_\ell x_\ell + \frac{\rho}{2} \|x_\ell - \bar{x}_\ell\|_{\Sigma_\ell}^2 \right\} - \lambda^\top b. \quad (28a)$$

$$\text{s.t. } c_\ell^E(x_\ell) = 0, c_\ell^I(x_\ell) + s_\ell = 0, \forall \ell \in \mathcal{R} \quad (28b)$$

return $\alpha_1 = \alpha_2 = 0$ and $\alpha_3 = \alpha_3^*$.

For the barrier problems (5), the globalization strategy [31, Alg. 3] is outlined in Algorithm 3 with the merit function defined as

$$\Phi(x) = \sum_{\ell \in \mathcal{R}} f_\ell(x_\ell) + \varepsilon_1 \left\| \sum_{\ell \in \mathcal{R}} A_\ell x_\ell - b \right\|_1 + \varepsilon_2 \sum_{\ell \in \mathcal{R}} \left\{ \left\| c_\ell^I(x_\ell) + s_\ell \right\|_1 + \left\| c_\ell^E(x_\ell) \right\|_1 \right\},$$

where the positive penalty pparameters $\varepsilon_1, \varepsilon_2$ are assumed to be sufficiently large such that Φ is an exact penalty function for the barrier problems (5).

ACKNOWLEDGMENT

The authors thank Frederik Zahn and François Pacaud for proofreading and discussion. This work was supported in part by the BMBF-project ENSURE III with grant number 03SFK1F0-3, in part by the Swiss National Science Foundation (SNSF) under the NCCR Automation project, grant agreement 51NF40_180545, and in part by the Swiss Federal Office of Energy's "SWEET" programme, and in part by BMWK via 03EI4057A (GrECCo).

REFERENCES

- [1] S. Frank and S. Rebennack, "An introduction to optimal power flow: Theory, formulation, and examples," *IEEE Trans.*, vol. 48, no. 12, pp. 1172–1197, 2016.
- [2] K. Lehmann, A. Grastien, and P. Van Hentenryck, "AC-feasibility on tree networks is NP-Hard," *IEEE Trans. Power Syst.*, vol. 31, no. 1, pp. 798–801, 2015.
- [3] D. Bienstock and A. Verma, "Strong NP-Hardness of AC power flows feasibility," *Oper. Res. Lett.*, vol. 47, no. 6, pp. 494–501, 2019.
- [4] T. Mühlpfordt, X. Dai, A. Engelmann, and V. Hagenmeyer, "Distributed power flow and distributed optimization—formulation, solution, and open source implementation," *Sustain. Energy, Grids Netw.*, vol. 26, p. 100471, 2021.
- [5] N. Patari, V. Venkataramanan, A. Srivastava, D. K. Molzahn, N. Li, and A. Annaswamy, "Distributed optimization in distribution systems: Use cases, limitations, and research needs," *IEEE Trans. Power Syst.*, vol. 37, no. 5, pp. 3469–3481, 2021.
- [6] D. K. Molzahn, F. Dörfler, H. Sandberg, S. H. Low, S. Chakrabarti, R. Baldick, and J. Lavaei, "A survey of distributed optimization and control algorithms for electric power systems," *IEEE Trans. Smart Grid*, vol. 8, no. 6, pp. 2941–2962, 2017.
- [7] T. Yang, X. Yi, J. Wu, Y. Yuan, D. Wu, Z. Meng, Y. Hong, H. Wang, Z. Lin, and K. H. Johansson, "A survey of distributed optimization," *Annu. Rev. Control*, vol. 47, pp. 278–305, 2019.
- [8] A. Al-Tawaha, E. Cibaku, S. Park, J. Lavaei, and M. Jin, "Distributed optimization and learning: A paradigm shift for power systems."
- [9] C. Lin, W. Wu, and M. Shahidehpour, "Decentralized AC optimal power flow for integrated transmission and distribution grids," *IEEE Trans. Smart Grid*, vol. 11, no. 3, pp. 2531–2540, 2020.
- [10] Q. Wang, C. Lin, W. Wu, B. Wang, G. Wang, H. Liu, H. Zhang, and J. Zhang, "A nested decomposition method for the AC optimal power flow of hierarchical electrical power grids," *IEEE Trans. Power Syst.*, 2022.
- [11] W. Zheng, W. Wu, B. Zhang, H. Sun, and Y. Liu, "A fully distributed reactive power optimization and control method for active distribution networks," *IEEE Trans. Smart Grid*, vol. 7, no. 2, pp. 1021–1033, 2015.
- [12] Q. Peng and S. H. Low, "Distributed optimal power flow algorithm for radial networks, i: Balanced single phase case," *IEEE Trans. Smart Grid*, vol. 9, no. 1, pp. 111–121, 2016.
- [13] A. Rajaei, S. Fattaheian-Dehkordi, M. Fotuhi-Firuzabad, and M. Moeini-Aghaie, "Decentralized transactive energy management of multi-microgrid distribution systems based on admm," *Int. J. Electr. Power Energy Syst.*, vol. 132, p. 107126, 2021.
- [14] S. Tu, A. Wächter, and E. Wei, "A two-stage decomposition approach for AC optimal power flow," *IEEE Trans. Power Syst.*, vol. 36, no. 1, pp. 303–312, 2020.
- [15] A. Engelmann, G. Stomberg, and T. Faulwasser, "An essentially decentralized interior point method for control," in *2021 60th IEEE/IEEE Conf. Decis. Control (CDC)*. IEEE, 2021, pp. 2414–2420.
- [16] X. Dai, J. Zhai, Y. Jiang, Y. Guo, C. N. Jones, and V. Hagenmeyer, "Advancing distributed ac optimal power flow for integrated transmission-distribution systems," *IEEE Trans. Network Sci. Eng.*, vol. 12, no. 1, pp. 1210 – 1223, 2025.
- [17] T. Erseghe, "Distributed optimal power flow using ADMM," *IEEE Trans. Power Syst.*, vol. 29, no. 5, pp. 2370–2380, 2014.
- [18] J. Guo, G. Hug, and O. K. Tonguz, "A case for nonconvex distributed optimization in large-scale power systems," *IEEE Trans. Power Syst.*, vol. 32, no. 5, pp. 3842–3851, 2017.
- [19] S. Mhanna, G. Verbič, and A. C. Chapman, "Adaptive ADMM for distributed AC optimal power flow," *IEEE Trans. Power Syst.*, vol. 34, no. 3, pp. 2025–2035, 2018.
- [20] K. Sun and X. A. Sun, "A two-level ADMM algorithm for AC OPF with global convergence guarantees," *IEEE Trans. Power Syst.*, vol. 36, no. 6, pp. 5271–5281, 2021.
- [21] —, "A two-level distributed algorithm for nonconvex constrained optimization," *Comput. Optim. Appl.*, vol. 84, no. 2, pp. 609–649, 2023.

- [22] A. Engelmann, T. Mühlpfordt, Y. Jiang, B. Houska, and T. Faulwasser, "Distributed AC optimal power flow using ALADIN," *IFAC-PapersOnLine*, vol. 50, no. 1, pp. 5536–5541, 2017.
- [23] A. Engelmann, Y. Jiang, T. Mühlpfordt, B. Houska, T. Faulwasser, "Toward Distributed OPF Using ALADIN," *IEEE Trans. Power Syst.*, vol. 34, no. 1, pp. 584–594, 2019.
- [24] A. Engelmann, Y. Jiang, B. Houska, and T. Faulwasser, "Decomposition of nonconvex optimization via bi-level distributed ALADIN," *IEEE Trans. Control Netw. Syst.*, vol. 7, no. 4, pp. 1848–1858, 2020.
- [25] X. Dai, A. Kocher, J. Kovačević, B. Dindar, Y. Jiang, C. Jones, H. K. Çakmak, and V. Hagenmeyer, "Ensuring data privacy in ac optimal power flow with a distributed co-simulation framework," *Electr. Power Syst. Res.*, vol. 235, p. 110710, 2024.
- [26] H. Sun, Q. Guo, B. Zhang, Y. Guo, Z. Li, and J. Wang, "Master-slave-splitting based distributed global power flow method for integrated transmission and distribution analysis," *IEEE Trans. Smart Grid*, vol. 6, no. 3, pp. 1484–1492, 2014.
- [27] A. X. Sun, D. T. Phan, and S. Ghosh, "Fully decentralized ac optimal power flow algorithms," in *2013 IEEE Power & Energy Society General Meeting*. IEEE, 2013, pp. 1–5.
- [28] J. Guo, G. Hug, and O. K. Tonguz, "Intelligent partitioning in distributed optimization of electric power systems," *IEEE Trans. Smart Grid*, vol. 7, no. 3, pp. 1249–1258, 2015.
- [29] R. D. Zimmerman, C. E. Murillo-Sánchez, and R. J. Thomas, "Matpower: Steady-state operations, planning, and analysis tools for power systems research and education," *IEEE Trans. Power Syst.*, vol. 26, no. 1, pp. 12–19, 2010.
- [30] S. Babaeinejadsarookolae, A. Birchfield, and et al, "The power grid library for benchmarking AC optimal power flow algorithms," *arXiv preprint arXiv:1908.02788*, 2019.
- [31] B. Houska, J. V. Frasch, and M. Diehl, "An augmented lagrangian based algorithm for distributed nonconvex optimization," *SIAM J. Optim.*, vol. 26, no. 2, pp. 1101–1127, 2016.
- [32] X. Dai, Y. Cai, Y. Jiang, and V. Hagenmeyer, "Rapid scalable distributed power flow with open-source implementation," *IFAC-PapersOnLine*, vol. 55, no. 13, pp. 145–150, 2022, 9th IFAC NECSYS 2022.
- [33] J. Nocedal and S. Wright, *Numerical optimization*. Springer Science & Business Media, 2006.
- [34] L. Lanza, T. Faulwasser, and K. Worthmann, "Distributed optimization for energy grids: A tutorial on ADMM and ALADIN," *arXiv preprint arXiv:2404.03946*, 2024.
- [35] A. Wächter and L. T. Biegler, "On the implementation of an interior-point filter line-search algorithm for large-scale nonlinear programming," *Math. Program.*, vol. 106, no. 1, pp. 25–57, 2006.
- [36] S. Shin, C. Coffrin, K. Sundar, and V. M. Zavala, "Graph-based modeling and decomposition of energy infrastructures," *IFAC-PapersOnLine*, vol. 54, no. 3, pp. 693–698, 2021.
- [37] Q. Tran Dinh, C. Savorgnan, and M. Diehl, "Combining lagrangian decomposition and excessive gap smoothing technique for solving large-scale separable convex optimization problems," *Computational Optimization and Applications*, vol. 55, no. 1, pp. 75–111, 2013.
- [38] R. H. Byrd, G. Liu, and J. Nocedal, "On the local behavior of an interior point method for nonlinear programming," *Numerical analysis*, vol. 1997, pp. 37–56, 1997.
- [39] D. P. Bertsekas, "Nonlinear programming," *J. Oper. Res. Soc.*, vol. 48, no. 3, pp. 334–334, 1997.
- [40] D. Bertsekas, "On the convergence properties of second-order multiplier methods," *J. Optim. Theory Appl.*, vol. 25, no. 3, pp. 443–449, 1978.
- [41] N. I. Gould, "On practical conditions for the existence and uniqueness of solutions to the general equality quadratic programming problem," *Math. Program.*, vol. 32, no. 1, pp. 90–99, 1985.
- [42] E. V. Haynsworth, "Determination of the inertia of a partitioned hermitian matrix," *Linear algebra and its applications*, vol. 1, no. 1, pp. 73–81, 1968.
- [43] F. Zhang, *The Schur complement and its applications*. Springer Science & Business Media, 2006, vol. 4.
- [44] A. Murray, M. Kyesswa, P. Schmurr, H. Çakmak, and V. Hagenmeyer, "On grid partitioning in AC optimal power flow," in *2020 IEEE PES ISGT (Europe)*. The Hague, Netherlands: IEEE, 2020, pp. 524–528.
- [45] A. Murray, M. Kyesswa, H. Çakmak, and V. Hagenmeyer, "On optimal grid partitioning for distributed optimization of reactive power dispatch," in *2021 IEEE Power & Energy Society Innovative Smart Grid Technologies Conference (ISGT)*. Washington, DC, USA: IEEE, 2021, pp. 1–5.
- [46] P. Sanders and C. Schulz, "Engineering multilevel graph partitioning algorithms," in *Algorithms–ESA 2011. 19th Annual European Symposium, Saarbrücken, Germany, September 5-9, 2011. Proceedings*. Ed.: C. Demetrescu. Saarbrücken, Germany: Springer Berlin Heidelberg, 2011, p. 469.
- [47] —, "Think Locally, Act Globally: Highly Balanced Graph Partitioning," in *Proceedings of the 12th International Symposium on Experimental Algorithms (SEA'13)*, ser. LNCS, vol. 7933. Springer, 2013, pp. 164–175.
- [48] A. Migdalas, P. M. Pardalos, and S. Storøy, *Parallel computing in optimization*. Springer Science & Business Media, 2013, vol. 7.
- [49] R. B. Schnabel, "A view of the limitations, opportunities, and challenges in parallel nonlinear optimization," *Parallel computing*, vol. 21, no. 6, pp. 875–905, 1995.
- [50] M. Colombo, A. Grothey, J. Hogg, K. Woodsend, and J. Gondzio, "A structure-conveying modelling language for mathematical and stochastic programming," *Math. Program. Comput.*, vol. 1, pp. 223–247, 2009.
- [51] J.-P. Watson, D. L. Woodruff, and W. E. Hart, "Pysp: modeling and solving stochastic programs in python," *Math. Program. Comput.*, vol. 4, pp. 109–149, 2012.
- [52] J. S. Rodriguez, R. B. Parker, C. D. Laird, B. L. Nicholson, J. D. Sirola, and M. L. Bynum, "Scalable parallel nonlinear optimization with pynumero and parapint," *INFORMS Journal on Computing*, vol. 35, no. 2, pp. 509–517, 2023.
- [53] J. Bradbury, R. Frostig, P. Hawkins, M. J. Johnson, C. Leary, D. Maclaurin, G. Necoara, A. Paszke, J. VanderPlas, S. Wanderman-Milne et al., "Jax: composable transformations of python+ numpy programs," 2018.
- [54] A. Paszke, S. Gross, F. Massa, A. Lerer, J. Bradbury, G. Chanan, T. Killeen, Z. Lin, N. Gimelshein, L. Antiga et al., "Pytorch: An imperative style, high-performance deep learning library," *Advances in neural information processing systems*, vol. 32, 2019.
- [55] S. Shin, M. Anitescu, and F. Pacaud, "Accelerating optimal power flow with gpus: Simd abstraction of nonlinear programs and condensed-space interior-point methods," *Electr. Power Syst. Res.*, vol. 236, p. 110651, 2024.
- [56] F. Pacaud, M. Schanen, S. Shin, D. A. Maldonado, and M. Anitescu, "Parallel interior-point solver for block-structured nonlinear programs on simd/gpu architectures," *Optimization Methods and Software*, pp. 1–24, 2024.
- [57] J. Kardoš, D. Kourounis, O. Schenk, and R. Zimmerman, "BELTISTOS: A robust interior point method for large-scale optimal power flow problems," *Electr. Power Syst. Res.*, vol. 212, p. 108613, 2022.
- [58] J. A. Andersson, J. Gillis, G. Horn, J. B. Rawlings, and M. Diehl, "Casadi: a software framework for nonlinear optimization and optimal control," *Math. Program. Comput.*, vol. 11, no. 1, pp. 1–36, 2019.
- [59] I. S. Duff, "Ma57—a code for the solution of sparse symmetric definite and indefinite systems," *ACM TOMS*, vol. 30, no. 2, pp. 118–144, 2004.
- [60] S. Fliscounakis, P. Panciatici, F. Capitanescu, and L. Wehenkel, "Contingency ranking with respect to overloads in very large power systems taking into account uncertainty, preventive, and corrective actions," *IEEE Trans. Power Syst.*, vol. 28, no. 4, pp. 4909–4917, 2013.
- [61] C. Josz, S. Fliscounakis, J. Maeght, and P. Panciatici, "AC power flow data in matpower and qcqp format: itesla, rte snapshots, and pegase," *arXiv preprint arXiv:1603.01533*, 2016.
- [62] I. Aravena, D. K. Molzahn, S. Zhang, C. G. Petra, F. E. Curtis, S. Tu, A. Wächter, E. Wei, E. Wong, A. Gholami et al., "Recent developments in security-constrained AC optimal power flow: Overview of challenge 1 in the arpa-e grid optimization competition," *Operations research*, vol. 71, no. 6, pp. 1997–2014, 2023.
- [63] J. M. Snodgrass, *Tractable algorithms for constructing electric power network models*. The University of Wisconsin-Madison, 2021.
- [64] Q. T. Dinh, I. Necoara, and M. Diehl, "A dual decomposition algorithm for separable nonconvex optimization using the penalty function framework," in *52nd IEEE CDC*. IEEE, 2013, pp. 2372–2377.